Benchmarking Electrocatalyst Stability for Acidic Oxygen Evolution Reaction The Crucial Role of Dissolved Ion Concentration

Wei, Chao; Wang, Zhenbin; Otani, Kanan; Hochfilzer, Degenhart; Zhang, Ke; Nielsen, Rasmus; Chorkendorff, Ib; Kibsgaard, Jakob

Published in:
ACS Catalysis

Published: 03/11/2023

Document Version:
Post-print, also known as Accepted Author Manuscript, Peer-reviewed or Author Final version

Published version (DOI):
10.1021/acscatal.3c03257

Publication details:
Wei, C., Wang, Z., Otani, K., Hochfilzer, D., Zhang, K., Nielsen, R., Chorkendorff, I., & Kibsgaard, J. (2023). Benchmarking Electrocatalyst Stability for Acidic Oxygen Evolution Reaction: The Crucial Role of Dissolved Ion Concentration. *ACS Catalysis*, *13*(21), 14058-14069. https://doi.org/10.1021/acscatal.3c03257

Benchmarking Electrocatalysts Stability for Acidic Oxygen Evolution Reaction: The Crucial Role of Dissolved Ion Concentration

Chao Wei[‡,1], *Zhenbin Wang*[‡,2,3], *Kanan Otani*[1,4], *Degenhart Hochfilzer*[1], *Ke Zhang*[1], *Rasmus Nielsen*[1], *Ib Chorkendorff*[1], *Jakob Kibsgaard*[*,1]

[1]Department of Physics, Technical University of Denmark, 2800 Kongens Lyngby, Denmark

[2]Department of Materials Science and Engineering, City University of Hong Kong, Hong Kong SAR, China

[3]School of Energy and Environment, City University of Hong Kong, Hong Kong SAR, China

[4]Department of Materials Science and Engineering, School of Materials and Chemical Technology, Tokyo Institute of Technology, 2121 Ookayama, Meguro-ku, Tokyo, 152-8552, Japan

KEYWORDS: oxygen evolution reaction, proton exchange membrane water electrolyzer, stability number, dissolved ion concentration, RuO_2, non-noble catalysts

ABSTRACT

Developing robust catalysts for the acidic oxygen evolution reaction (OER) is critical for large-scale implementation of proton exchange membrane (PEM) water electrolyzers. A promising strategy is to stabilize Ru-based catalysts by suppressing the Ru dissolution, which requires knowledge of the RuO_2 stability. This work explores the influences on measuring the stability number of RuO_2, and presents a comprehensive analysis and comparison of its stability with other electrocatalysts. We observe that RuO_2 shows relatively higher stability in electrolytes with a confined working volume because of the Nernst shift caused by the concentration buildup of dissolved Ru. The stability number of RuO_2 has a negligible dependence on the measurement duration, applied current density, Nafion content and substrate materials. Furthermore, we analyze the effects of these factors on other typical OER catalysts and identify that the concentration of dissolved ions is key to understanding the stability number measured by different electrochemical cells, and the claimed excellent stability of non-noble catalysts reported in the literature. In addition, the comparison of the stability number and intrinsic activity of RuO_2, IrO_2, and non-noble catalysts demonstrates that RuO_2 is at least two orders of magnitude less stable but also 10-fold more active than IrO_2, and that noble catalysts significantly outperform non-noble catalysts in terms of both stability and activity, posing a grand challenge in developing robust OER catalysts. This work establishes a baseline for enhancing the stability of Ru-based OER catalysts in acidic liquid cells and provides a valuable reference for PEM water electrolyzers.

Introduction

The scale-up implementation of proton exchange membrane (PEM) electrolyzers is primarily limited by the anodic reaction, i.e., oxygen evolution reaction (OER), because (i) the sluggish kinetics of OER dominates the energy loss associated with water splitting; and (ii) severe catalyst corrosion occurs under the extremely harsh OER conditions: acidic solution, highly oxidizing potential and O_2-abundant atmosphere.[1] These two challenges necessitate anode catalysts that are both catalytically active in enhancing energy efficiency, and stable in acidic media to ensure sustained efficiency over the lifespan of the electrolyzer. Currently, only Ir- and Ru-based oxides are considered qualified catalysts as they exhibit reasonable activities and stabilities for acidic OER.[1-2]

IrO_2 is the most reliable known acidic OER catalyst, but the scarcity of Ir hinders large-scale deployment of PEM electrolyzers,[1,3-5] requiring Ir loadings to be decreased from the current ~1 mg_{Ir} cm^{-2} to 0.05 mg_{Ir} cm^{-2} for gigawatt scale.[1,3,6] On the other hand, RuO_2 is more active (the intrinsic activity of RuO_2 is ~ 10 times higher than IrO_2),[7] but less stable than IrO_2;[8] the price of Ru is ~10 times (Jul 2023, fluctuating) cheaper than Ir, and the annual production of Ru is ~3 times higher than that of Ir.[9] Stabilizing RuO_2 offers a promising alternative for large-scale PEM electrolyzer applications.

Efforts to stabilize RuO_2 have led to an increased focus on measuring stability using accelerated stress tests (ASTs), such as chronopotentiometry (CP) or chronoamperometry (CA) measurement in rotating disk electrode (RDE) setup in acid liquid cells.[10-12] However, common problems exist that undermine the reliability of reported stability, particularly for discovering new catalysts with record-breaking stabilities surpassing RuO_2 or approaching IrO_2.

First, monitoring catalyst activity by current or potential over time does not necessarily reflect intrinsic stability of catalysts. For example, a temporal activity decay (e.g, a potential increase measured by CP), can also occur due to passivation of the supporting materials[13-17] or blockage of active sites caused by the oxygen microbubbles trapped within the catalyst layer.[11-12,18-19] Further, claimed stable or even improved activity in CP measurements might be due to the increasing roughness over time.[1] Second, the stability defined by CP/CA is only valid for an initial evaluation, as this method fails to directly capture catalyst dissolution,[1] which is an important metric for catalyst lifetime. Even though dissolution can be measured using inductively coupled plasma mass spectrometry (ICP-MS), the ICP-MS data alone is insufficient for comparing performance across different studies, due to the strong dependence of the dissolution rate on applied current or potential.[20] Normalizing the dissolved catalyst to total loading is a commonly used metric for stability comparison, but it does not reflect the catalyst lifetime, because the percentage of dissolved catalyst depends heavily on the catalyst loading. To address these limitations, researchers have developed improved metrics such as the stability number[20-21] and activity-stability factor,[22] which normalize the amount of evolved oxygen to dissolved catalyst. Third, the stability number is not a "stable" metric since external factors can influence its measurement, as demonstrated by meticulous work on IrO_x[21] and a recent perspective.[23] However, for RuO_2, the impact of experimental methods on measuring the stability number is unknown, which makes it difficult to determine whether a reported stability is due to inherent catalyst properties or external factors. Fourth, the inappropriate selection of a benchmark RuO_2 catalyst could falsely identify a stable catalyst. To prove a catalyst more stable than RuO_2, it is necessary to compare its stability number against that of RuO_2. Nevertheless, the choice of RuO_2 as the benchmark remains uncertain due to the existence of reported diverse

stability numbers for different RuO_2 materials.[20,24-27] Given these concerns, conducting a benchmark study to examine the impact of experimental parameters on the stability measurements of RuO_2 and providing an overview of the stability numbers of various OER catalysts would offer valuable guidance for future catalyst exploration.

In this work, we investigate factors influencing the measurement of the stability number of RuO_2 and established a benchmark for its stability number. Our findings reveal that when RuO_2 is present in a confined volume electrolyte, it exhibits a higher stability number due to the Nernst shift from the buildup of Ru concentration. Interestingly, we observe that the stability number of RuO_2 remains unaffected by the duration of measurement, applied current density/potential, Nafion content, and substrate materials. We further discuss the influence of these factors in relation to other catalysts and identify the concentration of dissolved ions as a key factor affecting the measured stability number. Finally, we underscore the pivotal tradeoff between stability and activity in the design of new OER catalysts, and conclude that current non-noble catalysts are unlikely to replace their noble counterparts under acidic conditions.

Results and discussion

Factors affecting the stability number measurement of RuO_2

This section delves into the factors that influence the stability number of RuO_2. These factors include the electrolyte volume, measurement time, applied current density/potential, Nafion content, and substrate materials.

A confined electrolyte volume facilitates the concentration buildup of dissolved Ru, yielding a higher stability number. To verify this hypothesis, we compared the stability numbers measured in our electrochemistry-mass spectrometry (EC-MS) setup,[28-29] which has an electrolyte volume of ~8 μl, (see volume estimation in Supporting Information, SI), with that of the conventional RDE method under 1600 rpm in an H-cell (separated by a Nafion membrane), where the electrolyte volume is 20 ml at the working electrode compartment (Figure 1a). The stability number measured in EC-MS is significantly higher than that in H-cell for six model RuO_2 catalysts, including powders and thin films prepared at different temperatures. For example, for Sigma-Aldrich RuO_2 the maximum difference is ~30 times. A smaller volume of electrolyte results in a higher concentration of Ru for the same amount of dissolved Ru, which in turn suppresses the dissolution of Ru, leading to a higher measured stability number. The accumulation of dissolved Ru leads to the stabilization of RuO_2, which can be rationalized by the Nernst shift and characterized qualitatively using the calculated aqueous stability based on the Pourbaix diagram. The Pourbaix diagram depicts the stability of chemical species, including solids and aqueous ions, through the redox reaction [reactants] + $aH_2O \rightarrow$ [products] + mH^+ + ne^-. The Nernst equation establishes the relationship between the Gibbs free energy of this reaction, pH, and cell potential. To describe the aqueous stability of a chemical species, the decomposition free energy (ΔG_{pbx})[30] is used, which is defined as the difference in Gibbs free energy between a target species and the most stable species at certain pH and external potential on the Pourbaix diagram. In essence, a larger ΔG_{pbx} indicates greater instability of the species. Figure 1b shows ΔG_{pbx} of RuO_2 as a function of applied potentials with Ru ion concentrations of 10^{-6} M and 10^{-4} M at pH = 1. The ion concentration of 10^{-6} M is conventionally used to assess the materials corrosion.[31-33] The ion concentration of 10^{-4} M was chosen for comparative stability

analysis because 3d transition metal oxides often exhibit dissolved ion concentration of ~10^{-4} M in experiment.[34-35] At a concentration of 10^{-6} M, the electrochemical stability window of RuO_2 spans from 0.62 V to 1.34 V, whereas at 10^{-4} M, it ranges from 0.52 V to 1.37 V, accompanied by a decrease in ΔG_{pbx} of 0.12 eV. The variation in the electrochemical stability window of RuO_2 within the OER regions is minimal, only 0.03 V, when compared to the overall change of 0.13 V. This can be attributed to the exceptional stability of RuO_2 in acidic solutions, particularly when compared to 3d transition metal oxides (see Figure 5d). Despite the small difference, the trend remains informative. RuO_2 becomes more stable at higher ion concentrations owing to the lowered ΔG_{pbx} (Nernst shift).

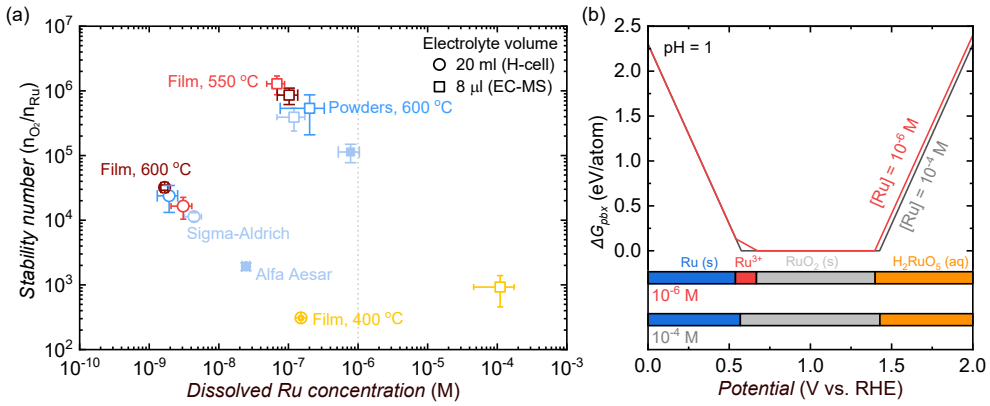

Figure 1. (a) The stability numbers of various RuO_2 catalysts versus the concentration of dissolved Ru, measured in H-cell (separated by Nafion membrane) and electrochemistry-mass spectrometry. All stability tests were performed by chronopotentiometry at 0.5 mA cm^{-2}_{geo} for 1 hour in 0.1 M $HClO_4$. The tested RuO_2 catalysts are thin films sputtered at 400 ºC, 550 ºC, and then further calcinated at 600 ºC; powders from Alfa-Aesar, Sigma-Aldrich, and those prepared by calcinating Sigma-Aldrich powders at 600 ºC. The vertical dashed line denotes 10^{-6} M, a common value for estimating material stability in Pourbaix diagrams. (b) Aqueous

decomposition free energy (ΔG_{pbx}) of RuO_2 with different Ru ion concentrations at pH = 1. The ΔG_{pbx} was derived from the experimental Pourbaix diagram.[36] The projection of ΔG_{pbx} onto the potential axis highlights the stable species at the corresponding potential.

Time span (within 1 h) does not affect stability number. We studied the influence of time span in stability number measurement (Figure 2a) by examining two metrics: cumulative and differential stability numbers, similar to "instantaneous" and "iterative" stability numbers brought up by a very recent perspective.[23] The cumulative stability number, such as at 60 min, is defined as $n_{O2(60\ min)}/n_{Ru(60\ min)}$, and the differential stability number at 60 min is $(n_{O2(60\ min)} - n_{O2(30\ min)})/(n_{Ru(60\ min)} - n_{Ru(30\ min)})$. The cumulative and differential stability numbers of RuO_2 in CP measurement remain unchanged and overlap as the measurement time increases (up to 60 min), implying that the duration of time is not a significant factor in estimating its stability number. This negligible effect of time span applies to other current densities as well (Figure 2a, inset). All measurements lasted for 1 hour, except for the CP measurement at 50 mA cm^{-2}_{geo}, which stopped after 30 min due to fast activity decay (Figure 2b). Based on a known stability number of 10^4 and an applied current density of 50 mA cm^{-2}_{geo} for 30 min, it is estimated that approximately 3 nm of the 25 nm-thick RuO_2 film was etched away. This result suggests that the activity decay is unlikely due to the loss of catalyst, but rather to the failure of the underlying substrate material, such as the 5 nm Ti adhesion layer or the glassy carbon. A similar observation was reported in a previous study,[13] where the potential in CP measurement increased exponentially to 2.3 V vs. RHE, despite the fact that only 1.3% of total loading was accounted for by the dissolved Ir.

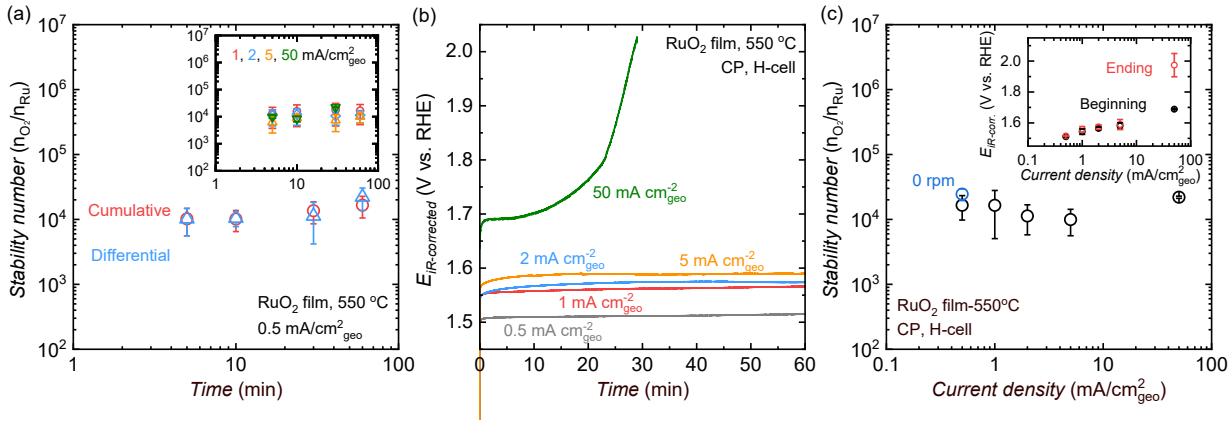

Figure 2. (a) The cumulative and differential stability number as a function of time span during chronopotentiometry (CP) measurement at 0.5 mA cm^{-2}_{geo}. Inset is the stability number (cumulative) as a function of time span at other current densities, normalized to the geometric area of electrode. (b) CP under various current densities. (c) Stability number as a function of applied current density, measured by CP for 1 hour. Inset shows the beginning and ending potentials. The beginning potential is defined as the value at 2 min of CP, while the ending potential is taken as that at 60 min, except for CP at 50 mA cm^{-2}_{geo}, where the ending potential is taken at 30 min. The catalysts are RuO_2 thin films sputtered at 550 °C. All measurements were performed in an H-cell, which has 20 ml 0.1 M $HClO_4$ electrolyte at the working electrode compartment, under 1600 rpm, except for blue data in panel (c).

Negligible influence of applied current density and rotation rate on stability number. The applied current density is a plausible variable for stability number estimation. We measured the stability number of RuO_2 as a function of (normalized) applied current density, as shown in

Figure 2c (Figure S1 and S2). The constant stability number of RuO_2 indicates that the stability number is not affected by the applied current density, which is also a reflection of potential (Figure 2c, inset). The rotation rate has no impact on the measurement of stability number, which is supported by the observation that the stability number of RuO_2 measured at a rotation rate of 0 rpm is identical to that measured at 1600 rpm (Figure 2c).

Negligible influence of Nafion content on stability number. The role of Nafion in measuring the stability number was studied by varying the Nafion content on two catalysts: Sigma-Aldrich RuO_2 powders and RuO_2 films synthesized at 550 ºC (Figure 3, S3). Measuring powder catalysts necessitates the use of Nafion as the binder to prevent the detachment of catalyst particles. However, Nafion may change the catalyst dissolution equilibrium by forming a polymer network that covers the catalyst surface and builds up the concentration of corrosion products. The stability number of both Sigma-Aldrich RuO_2 powders remains constant with different Nafion contents (Figure 3a), suggesting the negligible role of Nafion in stability number measurement. Similarly, when various loadings of Nafion cover the surface of RuO_2 film catalysts (Figure 3b), the stability number remains unchanged under both 0.5 and 5 mA cm^{-2}_{geo}. This finding also demonstrates that the Nafion binder plays a minor role. The observation is consistent with RuO_2 synthesized at 600 ºC (represented by the red data in Figure 3a), where sputtered films without Nafion exhibit the same stability number as powders with 23.5 wt% Nafion. This further indicates the limited influence of Nafion. It appears that the Nafion binder cannot create a confined space that affects Ru dissolution, possibly because the Nafion loading in rotating disk electrode (RDE) studies is not sufficiently high to form a thick Nafion layer. The investigated range of Nafion loading in this work is from 0 to 200 μg cm^{-2}_{geo}, encompassing the commonly

used values for RDE studies. Considering the known density of 2 g cm^{-3} for wet Nafion,[37] this loading (200 µg cm^{-2}_{geo}) corresponds to a nominal Nafion layer thickness of less than 1 µm.

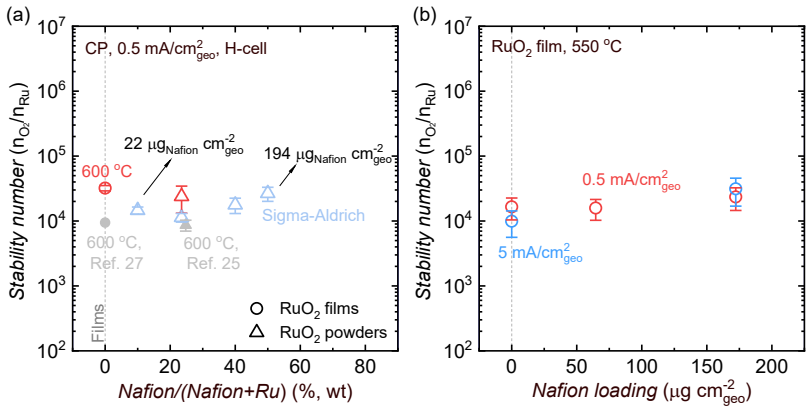

Figure 3. (a) The stability number of RuO_2 versus Nafion content (Nafion wt%, weight percentage), which is defined as Nafion/(Nafion + Ru). The RuO_2 loadings are maintained at 250 µg cm^{-2}_{geo}, while the Nafion loading ranges from 22 to 194 μg_{Nafion} cm^{-2}_{geo} (labelled with arrows). Stability number was measured by chronopotentiometry (CP) at 0.5 mA cm^{-2}_{geo} for 1 hour. Blue data are commercial RuO_2 powders from Sigma-Aldrich. Red data are RuO_2 films and powders prepared at 600 °C. Grey data are replotted from RuO_2 films[27] and powders[25] prepared at 600 °C. (b) Stability number of RuO_2 films (prepared at 550 °C) with different Nafion loadings. Nafion loading was controlled by drop-casting designated amount of Nafion solution on RuO_2 films. Stability number was measured by CP at 0.5 and 5 mA cm^{-2}_{geo} for 1 hour. In (a) (b), the data measured by this work was collected in an H-cell with a rotating disk electrode setup under 1600 rpm.

Substrate material does not influence the stability number of RuO_2 but is associated with the failure of electrode. To understand the role of a substrate material in stability measurements, we grew RuO_2 films on different substrates and studied their stability performance by examining two metrics: (1) potential decay (ΔE) extracted from CP measurement, a metric widely used for assessing catalyst stability in the literature and (2) stability number. The successful fabrication of conformal thin films is confirmed by XPS (X-ray photoelectron spectroscopy), as the underlying substrate material was not detected before or after OER (Figure 4, S4, S5). ΔE was defined as the difference between the ending potential taken at 60 min and the starting potential taken at 2 min (Figure S6). With different substrate materials supporting the RuO_2 films, ΔE varies with a range of ~150 mV (Figure 4a), while the stability numbers remain the same (Figure 4b). Similar observations were also reported for some powder catalyst[13,38] drop-casted on various substrates. This result indicates that ΔE correlates with the selected substrate material, independent of the catalyst (Figure S6d). In contrast, stability number is a reliable metric of intrinsic catalyst stability, unaffected by the substrate materials. The error bars for ΔE across multiple substrates are large, suggesting an intrinsic limitation in using ΔE (or CP) for stability estimation: it occasionally yields poor reproducibility. The variation of ΔE is likely due to the passivation of the substrate materials[13-17] and/or the presence of trapped bubbles within the catalyst layer,[11-12,18] rather than the catalyst itself. In particular, the exceptionally large ΔE of RuO_2/Au can be attributed to the passivation of substrate material. Instead of being beneath the RuO_2 film, the Au substrate is exposed after calcination (see XPS in Figure S7), which accelerates the passivation of Au to form Au oxide, and leads to the electrode failure.

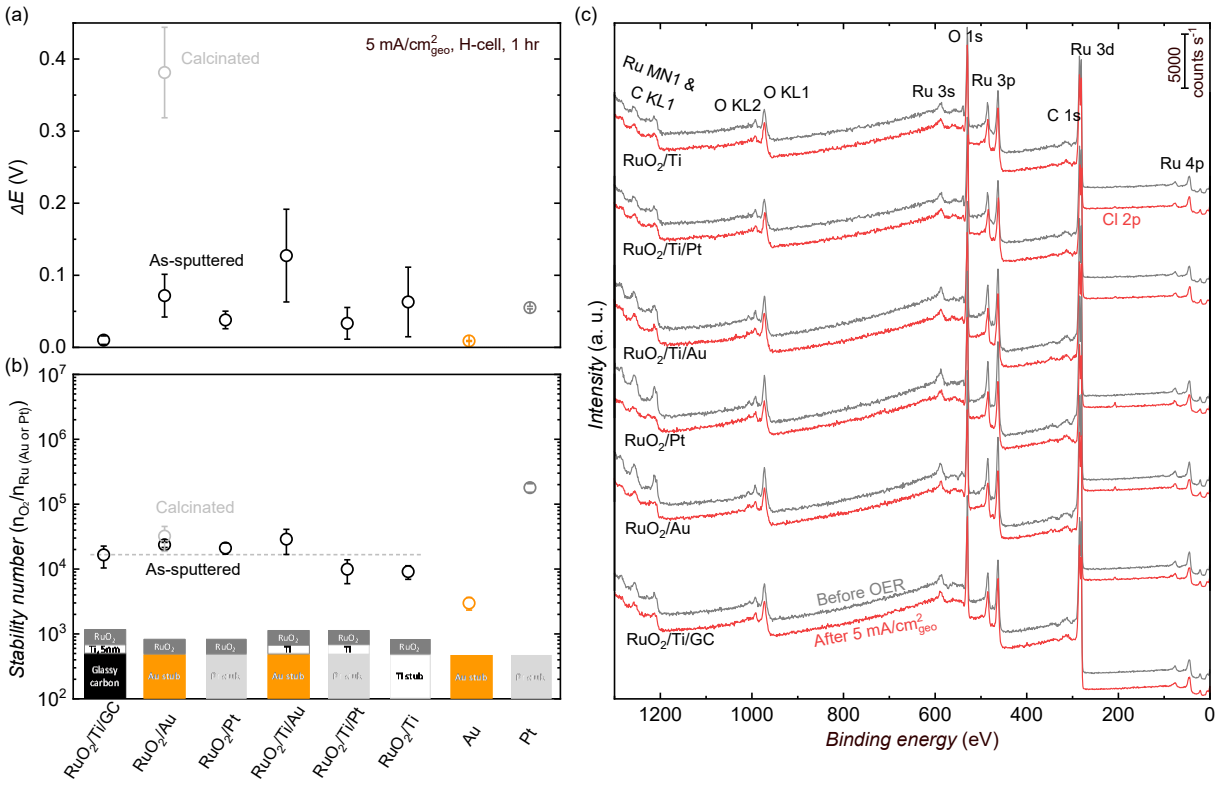

Figure 4. (a) The potential increase (ΔE) in chronopotentiometry (CP) measurement and (b) stability number of RuO_2 thin films (25 nm), deposited on various substrate materials by magnetron sputtering with the same sputtering conditions. CP was performed at 5 mA cm^{-2}_{geo} for 1 hour under 1600 rpm in an H-cell, which has 20 ml 0.1 M $HClO_4$ electrolyte at the working electrode compartment. The gray data denotes the electrode further calcinated at 600 °C in air. (c) X-ray photoelectron spectroscopy (XPS) spectra of RuO_2 films prepared at various substrate materials, before and after CP at 5 mA cm^{-2}_{geo} for 1 hour. The as-prepared RuO_2 films show the signal of Ru, O, and adventitious C, without showing the signal of the underlying substrate. After CP, an additional peak of Cl was observed, due to the residual electrolyte at catalyst surface.

Assessing the effect of studied factors for catalysts beyond RuO_2

Here, we compare our experimental findings on RuO_2 with other OER catalysts from the literature to emphasize the major influential factor: the concentration of dissolved ions.

Catalyst stabilization induced by the Nernst shift. Due to the accumulation of dissolved ions,[33] the Nernst shift can lead to an overestimation of the stability number, not only for RuO_2 but also for other catalyst materials, particularly 3d transition metal compounds.[34,39] For instance, measurements on Mn-based catalysts (e.g., MnO_2) commonly exhibit an Mn ion concentration of 10^{-4} M (corresponding to several ppm) and are reported to be stable under acidic OER.[34-35] To illustrate this concentration effect, we calculated the aqueous decomposition free energy (ΔG_{pbx}) of MnO_2 at two ion concentrations (10^{-6} M and 10^{-3} M) and pH = 2 (Figure 5a). At the higher ion concentration, MnO_2 shows a lower ΔG_{pbx} and much wider stable electrochemical window for OER, implying that the concentration would govern the Mn dissolution rate in a confined volume electrolyte. When comparing the stability of a new catalyst to that of a benchmark catalyst, such as IrO_2 or RuO_2, the concentration of dissolved metal ions should be taken into account, as it can stabilize the catalysts through the Nernst shift. This is particularly relevant for non-noble catalysts, which tend to exhibit significantly higher equilibrium concentrations of dissolved metal cations compared to noble ones.

Factors that increase the concentration of dissolved ions can directly affect the measured stability number. For example, high catalyst loading, long measurement time, addition of measured ions, can all impact stability, as discussed below. In a fuel cell setup, increasing the Pt loading can significantly decrease Pt dissolution, as a higher Pt loading creates a more porous catalyst layer, increasing local Pt concentration and reducing Pt dissolution.[40-41] In stark contrast, increasing the

IrO_x loading from 10 to 250 μg_{Ir} cm^{-2}_{geo} in OER has no impact on the stability number.[21] Although the stability number of RuO_2 is independent of measurement time within 1 hour CP (Figure 2), prolonging the measurement time can build up the concentration in an H-cell, ultimately affecting the measured stability number. In the CP measurement under 1 mA cm^{-2}_{geo} at $Ir_{50}Ti_{50}O_x$ OER catalyst, the concentration of dissolved Ir in 10 ml electrolyte remains constant after 200 min, which is attributed to the equilibrium of Ir dissolution in the used H-cell with 10 ml electrolyte in the anodic compartment (separated from the cathodic compartment by a fine glass grit).[42] The time required to reach dissolution equilibrium can vary depending on the type of catalysts and experimental conditions. For example, when testing IrO_x under 2 mA cm^{-2}_{geo} in 28 ml electrolyte,[21] equilibrium was not achieved even after 25 h. When Ir black was tested under 1.86 mA cm^{-2}_{geo} in 50 ml electrolyte,[13] the dissolution rate remains constant after 10 h. Similarly, in the case of RuO_2 tested under 2 mA cm^{-2}_{geo} in 20 ml electrolyte (Figure S8a), the dissolution equilibrium was not reached within 10 h. However, with RuSb binary oxide tested under 0.5 mA cm^{-2}_{geo} in 20 ml electrolyte (Figure S8c), the dissolution equilibrium was attained in ~15 min. According to the Nernst principle, intentionally adding metal cations to electrolyte can stabilize catalysts, such as in the case of the ternary Co-Fe-Pb oxides catalysts,[43-44] where the additions of Co^{2+}, Fe^{3+} and Pb^{2+} are essential for maintaining OER stability. An interesting observation is that adding 1 ug_{Ir} L^{-1} Ir cations into the electrolyte does not alter the stability number of IrO_x.[21] This lack of influence is likely because the concentration of added Ir cations is not sufficiently high to stabilize IrO_x. However, this hypothesis requires further validation. However, adding metal cations to the electrolyte is not practical for PEM electrolyzers, as these metal cations can have detrimental impact on the system:[3,45-47] i) metal cations diffuse into the membrane, resulting in a higher resistance; ii) migrate to the cathode and lead to deposition of

metal or precipitation of metal hydroxide, which in turn ruins the cathodic reaction; iii) the decomposition of H_2O_2 (chemically formed by the reaction of crossed-over H_2/O_2 at catalyst surface) can be promoted by metal cations, to generate radicals that accelerate membrane thinning.

Other factors overestimating stability number. The selection of time span can lead to different stability claims for a catalyst with a varying dissolution rate. Unlike RuO_2 catalyst, which has a constant dissolution rate (Figure 2a), other catalysts, such as $Ir_xRu_{1-x}O_y$,[25] $Y_2Ir_2O_7$,[48] $(Ru+Sb)O_x$,[49] $(Mn+Sb)O_x$,[49] IrO_x,[21] $Sr_{1.7}Ru_5Ir_1O_{13.7}$,[50] $SrIr_{0.8}Zn_{0.2}O_3$[23] and Ag_2BiO_x[51] show decreasing dissolution rates with increasing measurement time. In such cases, the stability number increases over time, making it challenging to determine stability by choosing between cumulative and differential stability number, as the latter is generally higher than the former.[23] It is important for readers to pay attention to whether the reported stability number is cumulative, as in the case of $Ir_xRu_{1-x}O_y$,[25] $Y_2Ir_2O_7$[48] and $Sr_{1.7}Ru_5Ir_1O_{13.7,}$[50] or differential, as in the case of $(Ru+Sb)O_x$,[49] $(Mn+Sb)O_x$,[49] IrO_x[21] and Ag_2BiO_x.[51]

Measurement time can overestimate stability number due to non-catalyst factors. For example, in a stagnant cell, the dissolution equilibrium can be achieved by a CP measurement that lasts too long, as demonstrated by $Ir_{0.5}Ti_{0.5}O_x$ catalyst.[42] The absorption or crossover of dissolved metal cations in the Nafion membrane (used to separate working and counter electrode compartment) can underestimate the ion concentration in working electrode compartment if the Nafion membrane is soaked in electrolyte for a prolonged measurement time. Storing Ru-containing electrolyte (several ppb Ru) in the H-cell working electrode compartment leads to a decrease of Ru concentration over time (Figure S9). A similar observation was reported in a previous study,

where immersing an 8 cm^2 Nafion membrane in a 500 ppb Ir solution (2.6 x 10^{-6} M) for 1 hour resulted in the intake of ~8% of the total Ir cations.[13] The use of Nafion membrane gradually absorbs dissolved ions, but the concentration of dissolved ions can also be underestimated if the membrane is omitted, because the dissolved metal cations can be deposited on the counter electrode in the absence of a separate compartment for the counter electrode.

The stability number of a catalyst may depend on the applied current density. Unlike RuO_2 (Figure 2c) or IrO_2 (Figure S10),[20] whose stability number is constant versus the applied current density, Ir metal shows a current density dependence. For Ir metal at a potential window > 1.8 V vs. RHE, a higher current density leads to a lower stability number.[20] This highlights the importance of considering the applied current density (or potential) as a variable when comparing the stability of different catalysts.

The disk rotation rate does not impact the stability number measurement. Specifically, the stability numbers of RuO_2, measured at rotation rates of 0 and 1600 rpm, are identical (Figure 2c). Since rotation rate reflects the mass transport of dissolved Ru, its negligible influence suggests that the diffusion rate of dissolved Ru is fast enough to vacate the catalyst surface without a buildup of local concentration near it. This finding is consistent with the observation of IrO_x, where altering the flow rate — which reflects mass transport — in an in-situ ICP flow cell does not affect the stability number.[21]

The impact of Nafion content on the stability number is under debate. Nafion appears to have a negligible effect on RuO_2 stability number. Similarly, IrO_x powders with Nafion and thin films exhibit identical stability number(Figure 5b);[20] IrO_2 powders calcinated at 600 ºC with Nafion show the same stability number as IrO_2 films calcinated at the same temperature (Figure

5b),[20,25,27] indicating Nafion does not affect the stability number. However, some studies report that Nafion can suppress catalyst dissolution by increasing the local concentration of dissolved species. For instance, increasing the Nafion content from 5 to 33 wt% enhances the stability number of IrO_x powders by about eight times, as shown in Figure 5b, ref [21], whereas further increasing the Nafion content to 50 wt% results in a slight decrease in the stability number. Additionally, a Nafion membrane layer added on top of the catalyst layer can reduce Pt dissolution by three-fold.[40] The role of Nafion in measuring stability number remains unsettled. Tentatively, we conclude that Nafion's contribution to stability number measurement is minor, at least for RuO_2. This, in turn, suggests that factors other than the ionomer (Nafion) are responsible for the higher stability number observed in MEA than in aqueous model systems.[20-21]

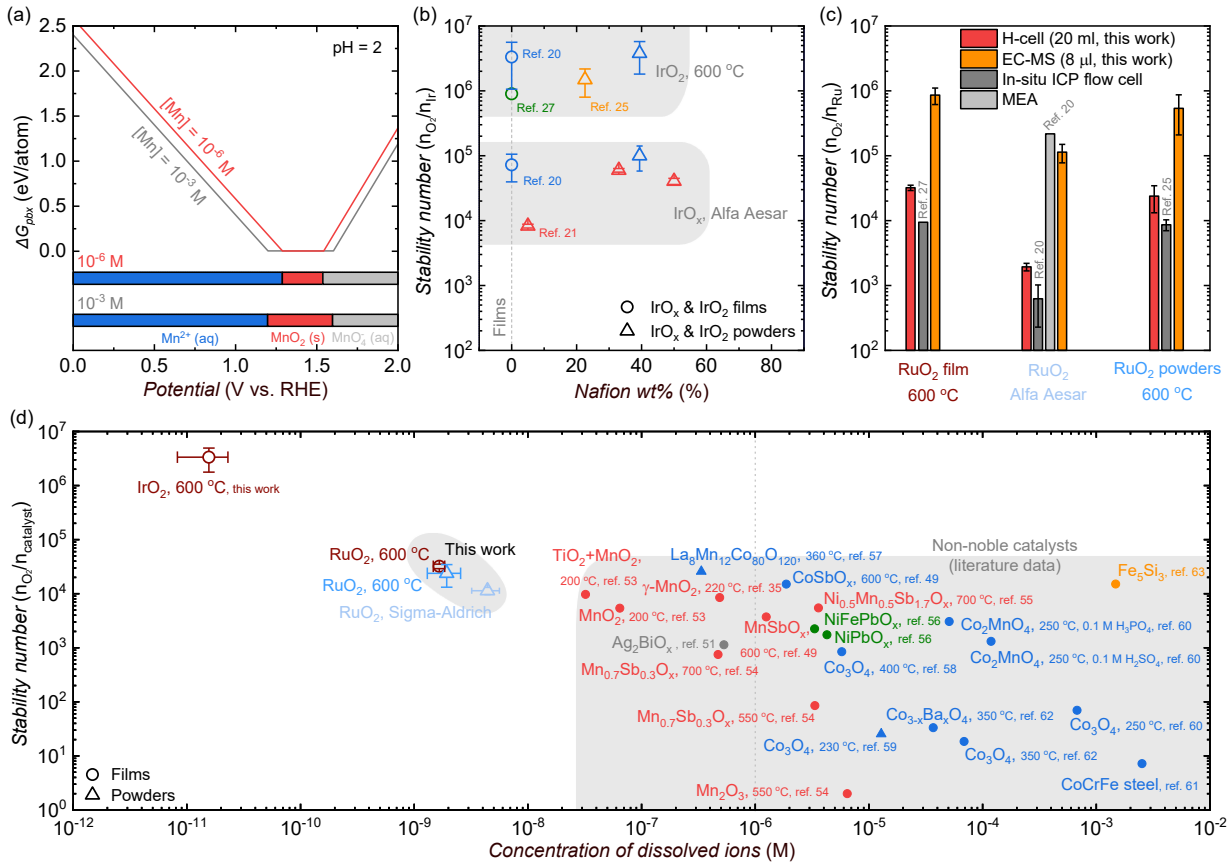

Figure 5. (a) Calculated aqueous decomposition free energy (ΔG_{pbx}) of Mn at different Mn ion concentrations, pH = 2. The ΔG_{pbx} was derived from the experimental Pourbaix diagram.[52] The projection of ΔG_{pbx} onto the potential axis highlights the stable species at corresponding potential. (b) A collection of literature data showing the stability number of IrO_x and IrO_2 versus Nafion content, which is defined as Nafion/(Nafion + Ir). The data includes: IrO_x film (prepared at room temperature),[20] IrO_x powders (Alfa Aesar),[20-21] IrO_2 films prepared at 600 °C,[20,27] IrO_2 powders prepared at 600 °C.[20,25] (c) The stability number of RuO_2 measured in different electrochemical cells. Red columns are data measured in this work by H-cell. Gray columns are data extracted from literature: RuO_2 film prepared at 600 °C,[27] Alfa-Aesar RuO_2 powders,[20] RuO_2 powders prepared at 600 °C,[25] measured with in-situ ICP flow cell, by long-term chronopotentiometry (CP), rather than transient CV, which gives ~10 times lower estimation of stability number[20] and membrane electrode assembly (MEA). Orange columns are data measured by EC-MS in this work. (d) The stability numbers of RuO_2, IrO_2 catalysts and non-noble catalysts versus the concentration of dissolved metal ions. RuO_2 and IrO_2 catalysts were measured by this work, CP at 0.5 mA cm^{-2}_{geo} in an H-cell, which has 20 ml 0.1 M $HClO_4$ electrolyte in the working electrode compartment. Data of non-noble catalysts are extracted from the following publications: TiO_2 + MnO_2, 200 °C, stability number normalized to Mn;[53] MnO_2, 200 °C;[53] γ-MnO_2, 220 °C;[35] $MnSbO_x$, 600 °C, normalized to Mn;[49] $Mn_{0.7}Sb_{0.3}O_x$, 700 °C, normalized to Mn;[54] $Mn_{0.7}Sb_{0.3}O_x$, 550 °C, normalized to Mn;[54] $Ni_{0.5}Mn_{0.5}Sb_{1.7}O_x$, 700 °C, normalized to Ni + Mn;[55] Mn_2O_3, 550 °C;[54] Ag_2BiO_x, normalized to Ag;[51] $NiFePbO_x$, normalized to Ni + Fe + Pb;[56] $NiPbO_x$, normalized to Ni + Pb;[56] $La_8Mn_{12}Co_{80}O_x$, 360 °C, normalized to Co;[57] $CoSbO_x$, 600 °C, normalized to Co;[49] Co_3O_4, 400 °C;[58] Co_3O_4, 230 °C;[59] Co_2MnO_4, 250 °C, 0.1 M H_3PO_4, normalized to Co;[60] Co_2MnO_4, 250 °C, 0.1 M H_2SO_4,

normalized to Co;[60] Co_3O_4, 250 °C;[60] CoCrFe steel;[61] $Co_{3-x}Ba_xO_4$, 350 °C, normalized to Co;[62] Co_3O_4, 350 °C;[62] Fe_5Si_3.[63] Detailed information about the experimental parameters of the literature data and data processing is provided in SI.

Concentration of dissolved ions is key to stability number estimation

Based on our experimental measurements and literature evidence, we can subsume various influential factors into one key factor: the concentration of dissolved ions. This finding facilitates the understanding of the stability number measured by various electrochemical cells, and the claimed excellent stability of non-noble catalysts.

Understanding the stability number measured by various electrochemical cells. By examining the stability numbers of the same catalyst measured by four different cells, we find that they follow the order of MEA ≈ EC-MS > H-cell ≈ in-situ ICP flow cell (Figure 5c). The key parameter to understand these measurements is the electrolyte volume, which can be quantified as follows. Our EC-MS has an extremely small working volume (~8 µl),[26,28-29] while the electrolyte volume of MEA is expected to be small due to the thick, porous catalyst layer with a high concentration of dissolved species.[21] The H-cell has a larger working volume of 20 ml and the electrolyte volume of the in-situ ICP flow cell[20-21,27] can be considered infinite due to the high flow rate that refreshes the working electrolyte volume. EC-MS thus resembles MEA (Figure 5c, see Alfa Aesar RuO_2) as both have a small working volume, and thus a high Ru concentration, resulting in a higher estimated stability number compared to H-cell and in-situ ICP flow cell. This observation is supported by the following: the stability number of IrO_x

measured by MEA (5 x 10^7) is ~3 orders of magnitude higher than that measured by the in-situ ICP flow cell (6 x 10^4) and H-cell (1 x 10^5,electrolyte volume 28 ml);[21,64] the stability number of RuO_2 (Alfa Aesar) in MEA is ~two orders of magnitude higher than in-situ ICP flow cell (replotted in Figure 5c)[20] and H-cell; and the stability number of RuO_2 in Figure 1a demonstrates that EC-MS gives a higher stability number than H-cell.

Regarding the higher stability number of MEA compared to acidic liquid cells (H-cell or in-situ ICP flow cell), previous studies[21] indicate there are several factors affecting the stability number. For instance, the stability number increases two orders of magnitude when altering the electrolyte from 0.1 M H_2SO_4 to deionized water in MEA. Considering MEA is measured at a higher temperature than acidic liquid cells, temperature would also have an impact on catalyst dissolution. For instance, the dissolution rate of Pt decreases from 25 to 65 ºC in 0.1 M H_2SO_4, but the variation falls within a factor of 2,[65] which is trivial compared with the substantial difference between acidic liquid cell and MEA (~3 orders of magnitude). While measurements undertaken within acidic liquid cells, such as the in-situ ICP flow cell, yield intrinsic catalyst stability, they ultimately underestimate catalyst stability under practical conditions within MEAs. This phenomenon is well-established with noble metal (i.e. Ir/Ru) catalysts. Therefore, non-noble metal catalysts might exhibit an enhanced stability within MEA devices compared to their performance in acidic liquid cells.

Comparing the stability number of the same material measured by H-cell and in-situ ICP flow cell (Figure 5c), we notice the stability number in an H-cell is 2~3 times higher than that in an in-situ ICP flow cell, consistent with earlier reports for Ir black,[13] IrO_x[21] and $Ir_{0.7}Sn_{0.3}O_x$.[27] This indicates a reasonable agreement between two approaches, further evidencing that in our

measurement using a stagnant cell with a 20 ml or larger electrolyte volume, the effect of Ru concentration buildup on the dissolution rate is negligible within 1 h. The cause for the 2∼3 times higher stability number in the H-cell compared to that in the flow cell is unknown. It is possible that this discrepancy is due to the absorption or crossover of metal ions into the Nafion membrane, which is utilized to separate the working and counter electrode compartment. Given that the electrochemical cell can influence the dissolution measurement and it is impractical to ensure that all laboratories follow the same method for measuring dissolution, we recommend that researchers reproduce the dissolution measurement of a standard catalyst (e.g., commercial product) to determine deviations caused by variation of laboratory practices.

Claimed excellent stability of non-noble catalysts. Based on our finding that a higher concentration of dissolved ions yields a higher measured stability number, we aim to raise awareness that the "excellent" stability of non-noble catalysts is likely because of the concentration buildup of dissolved ions. Figure 5d summarizes the literature data on the stability number of non-noble catalysts versus the concentration of dissolved ions, along with several RuO_2 catalysts measured in H-cell in this work for comparison. The stability numbers of non-noble catalysts are accompanied by much higher concentrations than that of RuO_2, indicating the high stability numbers of non-noble catalysts (some even comparable to RuO_2) are likely due to the stabilization effect of the Nernst shift stemming from the high concentration of dissolved ions. Additionally, the frequently observed long-lasting CP measurement of non-noble catalysts in acid liquid cells can be explained by this stabilization effect as well.

It is important to note that the reported stability numbers of non-noble catalysts presented in Figure 5d may not reflect their true intrinsic stability. This is because these numbers can be

overestimated due to the concentration buildup. It is hence necessary to verify this issue by conducting measurements using a large electrolyte volume or a constantly refreshed electrolyte. We want to caution that the data presented in Figure 5d are only intended to showcase literature progress and are not reliable for intrinsic stability analysis. The publications have at least one of the following weaknesses: the use of single-compartment cell which involves deposition at counter electrode, unspecified cell type or electrolyte volume, ion absorption/crossover caused by long-term use of Nafion membrane or glass frit. Most importantly, none of these works have provided the benchmark measurement of a standard catalyst. These weaknesses can lead to an overestimated stability number and an underestimated dissolved ion concentration.

Overviewing the stability numbers and intrinsic activities of Ru oxides, Ir oxides and non-noble catalysts

This section presents an overview of stability numbers and intrinsic activities of RuO_2, Ir-based, and non-noble catalysts. As the measurement conducted in 20 ml H-cell for 1 h can provide a representation of catalyst intrinsic stability, this method is used to assess a range of RuO_2 catalysts. By complementing these measurements with an analysis of examining literature data, we aim to gain in-depth insights into catalyst stability-activity.

Increasing the preparation temperature of RuO_2 significantly improves its stability number. Here, we prepared a set of RuO_2 thin film catalysts (see CP and materials characterizations in Figure S7, S11 – S17). Calcination at 600 ^oC results in the highest stability number, which is about two orders of magnitude higher than that of RuO_2 thin film prepared at 400 ^oC (Figure 6).

Similarly, calcinating Sigma Aldrich or Alfa Aesar RuO_2 powders at a higher temperature (≥ 600 ºC) also yields a higher stability number (e.g., ~10-fold enhancement over Alfa-Aesar RuO_2). This temperature-dependent stability highlights the importance of selecting a rational benchmark RuO_2 catalyst. Figure 6 also shows that the stability number of RuO_2 ranges from 10^2 to 10^4, which is at least two orders of magnitude less stable than the state-of-the-art catalyst, crystalline IrO_2. Enhancing the stability of RuO_2 can be effectively achieved through the utilization of the Nernst shift phenomenon. In addition to this approach, strategies involving the incorporation of Ru oxides with stable materials, such as Ir oxides,[25,66] hold great promise.

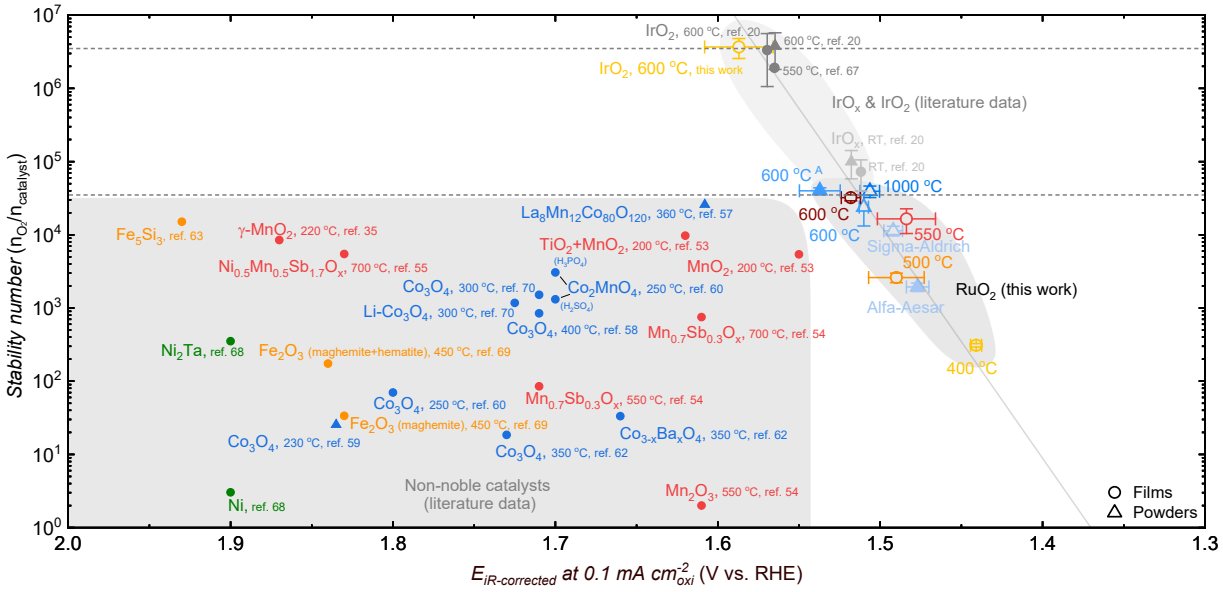

Figure 6. An overview of stability number of RuO_2 versus specific activity (the potential to reach the current density of 0.1 mA cm^{-2}_{oxi}, normalized to the surface area of catalysts), along with IrO_2 and IrO_x catalysts, and non-noble catalysts from literature. Data of IrO_2 film (600 ºC) in yellow color is measured by this work. Data of Ir-based catalysts in gray colors were originally reported as follows: IrO_2 film (600 ºC),[20] IrO_2 powders (600 ºC),[20] IrO_2 film (550

°C),[67] IrO_x film (RT, room temperature),[20] IrO_x powders (RT).[20] Detailed information about the experimental parameters of the literature data is provided in Tables S1 of the SI. Stability number measured in this work (RuO_2, various temperatures) are collected by chronopotentiometry (CP) under 1600 rpm for 1 h (0.5 mA cm^{-2}_{geo} for various RuO_2, and 5 mA cm^{-2}_{geo} for IrO_2 film 600 °C) in an H-cell which has 20 ml 0.1 M $HClO_4$ electrolyte in the working electrode compartment, and activities measured in this work are from electrochemistry-mass spectrometry. The two horizontal gray dashed lines denote the stability gap between Ru- and Ir-based catalysts. The dashed slash line denotes the stability-activity trade-off. Data of non-noble catalysts are extracted from the following publications: Fe_5Si_3, stability number normalized to Fe;[63] Ni_2Ta, normalized to Ni;[68] Ni;[68] γ-MnO_2, 220 °C;[35] $Ni_{0.5}Mn_{0.5}Sb_{1.7}O_x$, 700 °C, normalized to Ni + Mn;[55] Fe_2O_3 (maghemite + hematite), 450 °C;[69] Fe_2O_3 (maghemite), 450 °C;[69] $La_8Mn_{12}Co_{80}O_x$, 360 °C, normalized to Co;[57] Co_3O_4, 230 °C;[59] Co_3O_4, 250 °C;[60] Li-Co_3O_4, 300 °C, normalized to Co;[70] Co_3O_4, 300 °C;[70] Co_3O_4, 400 °C;[58] Co_2MnO_4, 250 °C, 0.1 M H_3PO_4, normalized to Co;[60] Co_2MnO_4, 250 °C, 0.1 M H_2SO_4, normalized to Co;[60] $Co_{3-x}Ba_xO_4$, 350 °C, normalized to Co;[62] Co_3O_4, 350 °C;[62] $Mn_{0.7}Sb_{0.3}O_x$, 550 °C, normalized to Mn;[54] $Mn_{0.7}Sb_{0.3}O_x$, 700 °C, normalized to Mn;[54] Mn_2O_3, 550 °C;[54] TiO_2 + MnO_2, 200 °C, normalized to Mn;[53] MnO_2, 200 °C.[53] Detailed information about the experimental parameters of the literature data and data processing is provided in SI.

Considering stability number only reflects catalyst stability, we plotted stability number as a function of intrinsic activity to study the stability-activity relationship. Intrinsic activity was defined as the potential to reach the current density of 0.1 mA cm^{-2}_{oxi}, normalized to the surface

area of oxide (estimated by double layer capacitance, Figure S2). Calcinating RuO_2 at a higher temperature gives better stability, but unfortunately lowers intrinsic activity. Increasing the synthesis temperature of RuO_2 thin films from 400 to 600 ^oC results in a ~100 times improvement in stability number, but ~10 times lower intrinsic activity (also see Figure S18). This decrease in intrinsic activity is further is accompanied by ~10 times decrease of roughness factor (Figure S2) due to high-temperature sintering. If we look at the geometric activity (current density normalized to geometric area of electrode, Figure S19), which is of great practical importance, the loss of both intrinsic activity and roughness factor further compromises this stability-activity tradeoff. A similar stability-activity trend has been observed for Ir-based catalysts as well: IrO_x prepared at room temperature displays ~10 times higher activity, but is 5~10 times less stable than rutile IrO_2 prepared at 600 ^oC (replotted in Figure 6 and Figure S20).[66-67,71-72] Note the stability numbers of Ir-based catalysts shown here are extracted from long-term CP/CA measurement, which gives ~10 times higher stability numbers than transient CV measurement.[20] By putting the intrinsic stability-activity relationship of both Ru- and Ir-based catalysts together (Figure 6), we observe that these two classes of catalysts follow exactly the same trend, implying the stability and activity might share the same descriptor, probably oxygen binding energy. We hope that this stability-activity trend can be further confirmed by plotting more literature data. As of now, only a limited number of works report both reliable assessment of intrinsic stability and activity. This stability-activity trend also highlights the challenging tradeoff involved in designing acidic OER catalysts, i.e., the stability-activity dilemma,[22,73] wherein improving one property comes at the cost of sacrificing the other.

By incorporating non-noble catalysts into the stability-activity plot, we emphasize the disparity in activity and stability between noble and non-noble catalysts. To extract the stability number

and intrinsic activity from literature, it is necessary to have certain information, including the concentration of dissolved ions, electrolyte volume, catalyst surface area, etc. However, this information has only been provided by a limited number of studies, as detailed in SI. It should be noted that the data of non-noble catalyst presented in this study are only to show a qualitative trend, as the stability number and intrinsic activity of these data are largely overestimated. The stability number has been overestimated because of the high concentration of dissolved ions that stabilize catalysts, and other weaknesses summarized in the previous discussions (see Figure 5d). The intrinsic activity has been overestimated because the measurements lack quantification of the produced O_2. Although the OER faradaic efficiency measured by on-line gas chromatography (GC) is commonly used to confirm the activity measured CV, the GC measurement during steady-state CP/CA does not necessarily reflect the activity derived from CV. This is because CV is a transient measurement technique involving the uncorrected current contributed by the catalyst background, catalyst dissolution (dissolution during CV is ~10 times[20] faster than steady-state CP), oxidation of carbon species initially adsorbed on catalyst surface. Even though the presented data points for non-noble catalysts are mostly overestimated, Figure 6 provides compelling evidence that, to this date, non-noble catalysts are not as effective as noble ones, particularly IrO_2, in terms of both stability and activity. Therefore, for any claims of developing an earth-abundant catalyst that can replace noble catalysts for acidic OER, it is crucial to have rigorous measurements of both stability number and intrinsic activity to provide sufficient support.

Ultimately, the critical question arises as to whether one can rely on a poor catalyst that is cheap for practical applicability. The poor activity of non-noble catalysts necessitates significantly higher overpotentials when compared to noble catalysts, leading to a substantial increase in

energy costs. This rise in energy expenses is probably more crucial than the actual catalyst cost itself. Non-noble catalysts are primarily sought after due to their low cost and abundance. However, these catalysts exhibit a considerably higher equilibrium concentration of dissolved ions (>10^3 higher than noble metal ions, Figure 5d), resulting in a significant increase in their usage and subsequent capital costs. Furthermore, closed loop recycling business models are more challenging using non-noble catalysts. Consequently, their implementation becomes less economically attractive, despite their abundance. Moreover, the poor stability of non-noble catalysts leads to a much faster catalyst leaching during electrolysis. The metal cations produced during this dissolution process can disrupt the operation of electrolyzers by damaging the membrane and cathode reactions, not only in water splitting electrolyzer for HER (as discussed in section 3), but also in cathode processes of other electrolyzers coupled with OER, such as H_2O_2 production[74] and CO/CO_2 reduction.[75]

Conclusions

We have investigated the possible influences on the measurement of stability numbers for RuO_2 catalysts. We find that because of the Nernst shift caused by the concentration buildup of dissolved Ru, a higher Ru concentration gives a higher stability number. The stability number of RuO_2 is constant versus the measurement time span, independent of the applied current density, Nafion content and substrate materials. The concentration of dissolved ions is identified as the key factor for understanding the stability measured by various electrochemical cells, and the claimed excellent stability of non-noble catalysts. By measuring various RuO_2 powders and films catalysts, we have benchmarked that the stability number of RuO_2 is at least ~100 times

less stable than IrO_2. The stability-activity correlation highlights the stability-activity dilemma and the irreplaceable status of noble catalysts in acidic OER. This work provides a baseline of measuring the stability of Ru-based OER catalysts in acidic liquid cells.

ASSOCIATED CONTENT

Supporting Information. The Supporting Information is available free of charge on the ACS Publications website at DOI: XXXXX. Detailed description of experimental protocols, including catalyst preparation (film and powder), ink recipe, electrochemical measurement in H-cell and EC-MS, ICP-MS measurement, materials characterization. Supplementary ICP-MS data, stability number results, electrochemistry data (CP, ECSA measurement, activity, EC-MS results), XPS and ISS data, SEM images.

The following files are available free of charge.

Supplementary data1, Data for Figure5d and 6 (Excel)

Supplementary data2, Extracting data for Figure5d and 6 (Excel in Zip)

AUTHOR INFORMATION

Corresponding Author

*Jakob Kibsgaard – Department of Physics, Technical University of Denmark, 2800 Kongens Lyngby, Denmark; Email: jkib@fysik.dtu.dk

Author Contributions

‡C.W. and Z.W. contributed equally to this work.

Notes

The authors declare no competing financial interest.

ACKNOWLEDGMENT

The authors thank Jacqueline McAnulty and Brian Peter Knudsen for the tremendous efforts on measuring and troubleshooting ICP-MS. We thank Jakob Ejler Sørensen for troubleshooting XPS. We gratefully acknowledge the funding by Villum Fonden, part of the Villum Center for the Science of Sustainable Fuels and Chemicals (V-SUSTAIN grant 9455). Z. W. acknowledges the funding support from City University of Hong Kong Start-up Grant 9020004.

REFERENCES

(1) Kibsgaard, J.; Chorkendorff, I., Considerations for the scaling-up of water splitting catalysts. *Nat. Energy* **2019,** *4*, 430-433.

(2) Seh, Z. W.; Kibsgaard, J.; Dickens, C. F.; Chorkendorff, I.; Nørskov, J. K.; Jaramillo, T. F., Combining theory and experiment in electrocatalysis: Insights into materials design. *Science* **2017,** *355*, eaad4998.

(3) Babic, U.; Suermann, M.; Büchi, F. N.; Gubler, L.; Schmidt, T. J., Critical Review—Identifying Critical Gaps for Polymer Electrolyte Water Electrolysis Development. *J. Electrochem. Soc.* **2017,** *164*, F387-F399.

(4) Bernt, M.; Hartig-Weiß, A.; Tovini, M. F.; El-Sayed, H. A.; Schramm, C.; Schröter, J.; Gebauer, C.; Gasteiger, H. A., Current Challenges in Catalyst Development for PEM Water Electrolyzers. *Chem. Ing. Tech.* **2020,** *92*, 31-39.

(5) Zheng, Y.-R.; Vernieres, J.; Wang, Z.; Zhang, K.; Hochfilzer, D.; Krempl, K.; Liao, T.-W.; Presel, F.; Altantzis, T.; Fatermans, J.; Scott, S. B.; Secher, N. M.; Moon, C.; Liu, P.; Bals, S.; Van Aert, S.; Cao, A.; Anand, M.; Nørskov, J. K.; Kibsgaard, J.; Chorkendorff, I., Monitoring oxygen production on mass-selected iridium–tantalum oxide electrocatalysts. *Nat. Energy* **2022,** *7*, 55-64.

(6) Bernt, M.; Siebel, A.; Gasteiger, H. A., Analysis of Voltage Losses in PEM Water Electrolyzers with Low Platinum Group Metal Loadings. *J. Electrochem. Soc.* **2018,** *165*, F305-F314.

(7) Lee, Y.; Suntivich, J.; May, K. J.; Perry, E. E.; Shao-Horn, Y., Synthesis and Activities of Rutile IrO2 and RuO2 Nanoparticles for Oxygen Evolution in Acid and Alkaline Solutions. *J. Phys. Chem. Lett.* **2012,** *3*, 399-404.

(8) Cherevko, S.; Geiger, S.; Kasian, O.; Kulyk, N.; Grote, J.-P.; Savan, A.; Shrestha, B. R.; Merzlikin, S.; Breitbach, B.; Ludwig, A.; Mayrhofer, K. J. J., Oxygen and hydrogen evolution reactions on Ru, RuO2, Ir, and IrO2 thin film electrodes in acidic and alkaline electrolytes: A comparative study on activity and stability. *Catal. Today* **2016,** *262*, 170-180.

(9) Vesborg, P. C. K.; Jaramillo, T. F., Addressing the terawatt challenge: scalability in the supply of chemical elements for renewable energy. *RSC Adv.* **2012,** *2*, 7933-7947.

(10) Risch, M., Upgrading the detection of electrocatalyst degradation during the oxygen evolution reaction. *Curr. Opin. Electrochem.* **2023,** *38*, 101247.

(11) El-Sayed, H. A.; Weiß, A.; Olbrich, L. F.; Putro, G. P.; Gasteiger, H. A., OER Catalyst Stability Investigation Using RDE Technique: A Stability Measure or an Artifact? *J. Electrochem. Soc.* **2019,** *166*, F458-F464.

(12) Fathi Tovini, M.; Hartig-Weiß, A.; Gasteiger, H. A.; El-Sayed, H. A., The Discrepancy in Oxygen Evolution Reaction Catalyst Lifetime Explained: RDE vs MEA - Dynamicity within the Catalyst Layer Matters. *J. Electrochem. Soc.* **2021,** *168*, 014512.

(13) Geiger, S.; Kasian, O.; Mingers, A. M.; Nicley, S. S.; Haenen, K.; Mayrhofer, K. J. J.; Cherevko, S., Catalyst Stability Benchmarking for the Oxygen Evolution Reaction: The Importance of Backing Electrode Material and Dissolution in Accelerated Aging Studies. *ChemSusChem* **2017,** *10*, 4140-4143.

(14) Oh, H.-S.; Nong, H. N.; Reier, T.; Bergmann, A.; Gliech, M.; Ferreira de Araújo, J.; Willinger, E.; Schlögl, R.; Teschner, D.; Strasser, P., Electrochemical Catalyst–Support Effects and Their Stabilizing Role for IrOx Nanoparticle Catalysts during the Oxygen Evolution Reaction. *J. Am. Chem. Soc.* **2016,** *138*, 12552-12563.

(15) Han, B.; Risch, M.; Belden, S.; Lee, S.; Bayer, D.; Mutoro, E.; Shao-Horn, Y., Screening Oxide Support Materials for OER Catalysts in Acid. *J. Electrochem. Soc.* **2018,** *165*, F813-F820.

(16) Edgington, J.; Deberghes, A.; Seitz, L. C., Glassy Carbon Substrate Oxidation Effects on Electrode Stability for Oxygen Evolution Reaction Catalysis Stability Benchmarking. *ACS Appl. Energy Mater.* **2022,** *5*, 12206-12218.

(17) Iwakura, C.; Inai, M.; Manabe, M.; Tamura, H., The cause of the activity loss of titanium-supported ruthenium dioxide electrodes during the anodic evolution of oxygen. *Denki Kagaku Oyobi Kogyo Butsuri Kagaku* **1980,** *48*, 91-96.

(18) Lazaridis, T.; Stühmeier, B. M.; Gasteiger, H. A.; El-Sayed, H. A., Capabilities and limitations of rotating disk electrodes versus membrane electrode assemblies in the investigation of electrocatalysts. *Nat. Catal.* **2022,** *5*, 363-373.

(19) Jovanovič, P.; Stojanovski, K.; Bele, M.; Dražić, G.; Koderman Podboršek, G.; Suhadolnik, L.; Gaberščček, M.; Hodnik, N., Methodology for Investigating Electrochemical Gas Evolution Reactions: Floating Electrode as a Means for Effective Gas Bubble Removal. *Anal. Chem.* **2019,** *91*, 10353-10356.

(20) Geiger, S.; Kasian, O.; Ledendecker, M.; Pizzutilo, E.; Mingers, A. M.; Fu, W. T.; Diaz-Morales, O.; Li, Z.; Oellers, T.; Fruchter, L.; Ludwig, A.; Mayrhofer, K. J. J.; Koper, M. T. M.; Cherevko, S., The stability number as a metric for electrocatalyst stability benchmarking. *Nat. Catal.* **2018,** *1*, 508-515.

(21) Knöppel, J.; Möckl, M.; Escalera-López, D.; Stojanovski, K.; Bierling, M.; Böhm, T.; Thiele, S.; Rzepka, M.; Cherevko, S., On the limitations in assessing stability of oxygen evolution catalysts using aqueous model electrochemical cells. *Nat. Commun.* **2021,** *12*, 2231-2239.

(22) Kim, Y.-T.; Lopes, P. P.; Park, S.-A.; Lee, A. Y.; Lim, J.; Lee, H.; Back, S.; Jung, Y.; Danilovic, N.; Stamenkovic, V.; Erlebacher, J.; Snyder, J.; Markovic, N. M., Balancing activity, stability and conductivity of nanoporous core-shell iridium/iridium oxide oxygen evolution catalysts. *Nat. Commun.* **2017,** *8*, 1449.

(23) Edgington, J.; Seitz, L. C., Advancing the Rigor and Reproducibility of Electrocatalyst Stability Benchmarking and Intrinsic Material Degradation Analysis for Water Oxidation. *ACS Catal.* **2023,** *13*, 3379-3394.

(24) Hubert, M. A.; Patel, A. M.; Gallo, A.; Liu, Y.; Valle, E.; Ben-Naim, M.; Sanchez, J.; Sokaras, D.; Sinclair, R.; Nørskov, J. K.; King, L. A.; Bajdich, M.; Jaramillo, T. F., Acidic Oxygen Evolution Reaction Activity–Stability Relationships in Ru-Based Pyrochlores. *ACS Catal.* **2020,** *10*, 12182-12196.

(25) Escalera-López, D.; Czioska, S.; Geppert, J.; Boubnov, A.; Röse, P.; Saraçi, E.; Krewer, U.; Grunwaldt, J.-D.; Cherevko, S., Phase- and Surface Composition-Dependent Electrochemical Stability of Ir-Ru Nanoparticles during Oxygen Evolution Reaction. *ACS Catal.* **2021,** *11*, 9300-9316.

(26) Scott, S. B.; Sørensen, J. E.; Rao, R. R.; Moon, C.; Kibsgaard, J.; Shao-Horn, Y.; Chorkendorff, I., The low overpotential regime of acidic water oxidation part II: trends in metal and oxygen stability numbers. *Energy Environ. Sci.* **2022,** *15*, 1988-2001.

(27) Kasian, O.; Geiger, S.; Mayrhofer, K. J. J.; Cherevko, S., Electrochemical On-line ICP-MS in Electrocatalysis Research. *Chem. Rec.* **2019,** *19*, 2130-2142.

(28) Trimarco, D. B.; Scott, S. B.; Thilsted, A. H.; Pan, J. Y.; Pedersen, T.; Hansen, O.; Chorkendorff, I.; Vesborg, P. C. K., Enabling real-time detection of electrochemical desorption phenomena with sub-monolayer sensitivity. *Electrochim. Acta* **2018,** *268*, 520-530.

(29) Scott, S. B.; Rao, R. R.; Moon, C.; Sørensen, J. E.; Kibsgaard, J.; Shao-Horn, Y.; Chorkendorff, I., The low overpotential regime of acidic water oxidation part I: the importance of O2 detection. *Energy Environ. Sci.* **2022,** *15*, 1977-1987.

(30) Singh, A. K.; Zhou, L.; Shinde, A.; Suram, S. K.; Montoya, J. H.; Winston, D.; Gregoire, J. M.; Persson, K. A., Electrochemical Stability of Metastable Materials. *Chem. Mater.* **2017,** *29*, 10159-10167.

(31) Wang, Z.; Guo, X.; Montoya, J.; Nørskov, J. K., Predicting aqueous stability of solid with computed Pourbaix diagram using SCAN functional. *npj Comput. Mater.* **2020,** *6*, 160.

(32) Peng, J.; Giordano, L.; Davenport, T. C.; Shao-Horn, Y., Stability Design Principles of Manganese-Based Oxides in Acid. *Chem. Mater.* **2022,** *34*, 7774-7787.

(33) Cherevko, S., Stabilization of non-noble metal electrocatalysts for acidic oxygen evolution reaction. *Curr. Opin. Electrochem.* **2023**, 101213.

(34) Pan, S.; Li, H.; Liu, D.; Huang, R.; Pan, X.; Ren, D.; Li, J.; Shakouri, M.; Zhang, Q.; Wang, M.; Wei, C.; Mai, L.; Zhang, B.; Zhao, Y.; Wang, Z.; Graetzel, M.; Zhang, X., Efficient and stable noble-metal-free catalyst for acidic water oxidation. *Nat. Commun.* **2022,** *13*, 2294.

(35) Li, A.; Ooka, H.; Bonnet, N.; Hayashi, T.; Sun, Y.; Jiang, Q.; Li, C.; Han, H.; Nakamura, R., Stable Potential Windows for Long-Term Electrocatalysis by Manganese Oxides Under Acidic Conditions. *Angew. Chem., Int. Ed.* **2019,** *58*, 5054-5058.

(36) Rard, J. A., Chemistry and thermodynamics of ruthenium and some of its inorganic compounds and aqueous species. *Chem. Rev.* **1985,** *85*, 1-39.

(37) Zook, L. A.; Leddy, J., Density and Solubility of Nafion: Recast, Annealed, and Commercial Films. *Anal. Chem.* **1996,** *68*, 3793-3796.

(38) Zlatar, M.; Nater, D.; Escalera-López, D.; Joy, R. M.; Pobedinskas, P.; Haenen, K.; Copéret, C.; Cherevko, S., Evaluating the stability of Ir single atom and Ru atomic cluster oxygen evolution reaction electrocatalysts. *Electrochim. Acta* **2023,** *444*, 141982.

(39) Wang, Z.; Zheng, Y.-R.; Montoya, J.; Hochfilzer, D.; Cao, A.; Kibsgaard, J.; Chorkendorff, I.; Nørskov, J. K., Origins of the Instability of Nonprecious Hydrogen Evolution Reaction Catalysts at Open-Circuit Potential. *ACS Energy Lett.* **2021,** *6*, 2268-2274.

(40) Ehelebe, K.; Knöppel, J.; Bierling, M.; Mayerhöfer, B.; Böhm, T.; Kulyk, N.; Thiele, S.; Mayrhofer, K. J. J.; Cherevko, S., Platinum Dissolution in Realistic Fuel Cell Catalyst Layers. *Angew. Chem., Int. Ed.* **2021,** *60*, 8882-8888.

(41) Keeley, G. P.; Cherevko, S.; Mayrhofer, K. J. J., The Stability Challenge on the Pathway to Low and Ultra-Low Platinum Loading for Oxygen Reduction in Fuel Cells. *ChemElectroChem* **2016,** *3*, 51-54.

(42) Kasian, O.; Li, T.; Mingers, A. M.; Schweinar, K.; Savan, A.; Ludwig, A.; Mayrhofer, K., Stabilization of an iridium oxygen evolution catalyst by titanium oxides. *Journal of Physics: Energy* **2021,** *3*, 034006.

(43) Chatti, M.; Gardiner, J. L.; Fournier, M.; Johannessen, B.; Williams, T.; Gengenbach, T. R.; Pai, N.; Nguyen, C.; MacFarlane, D. R.; Hocking, R. K.; Simonov, A. N., Intrinsically stable in situ generated electrocatalyst for long-term oxidation of acidic water at up to 80 °C. *Nat. Catal.* **2019,** *2*, 457-465.

(44) Simondson, D.; Chatti, M.; Bonke, S. A.; Tesch, M. F.; Golnak, R.; Xiao, J.; Hoogeveen, D. A.; Cherepanov, P. V.; Gardiner, J. L.; Tricoli, A.; MacFarlane, D. R.; Simonov, A. N., Stable

Acidic Water Oxidation with a Cobalt–Iron–Lead Oxide Catalyst Operating via a Cobalt-Selective Self-Healing Mechanism. *Angew. Chem., Int. Ed.* **2021,** *60*, 15821-15826.

(45) Grigoriev, S. A.; Dzhus, K. A.; Bessarabov, D. G.; Millet, P., Failure of PEM water electrolysis cells: Case study involving anode dissolution and membrane thinning. *Int. J. Hydrogen. Energ* **2014,** *39*, 20440-20446.

(46) Sun, S.; Shao, Z.; Yu, H.; Li, G.; Yi, B., Investigations on degradation of the long-term proton exchange membrane water electrolysis stack. *J. Power Sources* **2014,** *267*, 515-520.

(47) Weiß, A.; Siebel, A.; Bernt, M.; Shen, T. H.; Tileli, V.; Gasteiger, H. A., Impact of Intermittent Operation on Lifetime and Performance of a PEM Water Electrolyzer. *J. Electrochem. Soc.* **2019,** *166*, F487-F497.

(48) Hubert, M. A.; Gallo, A.; Liu, Y.; Valle, E.; Sanchez, J.; Sokaras, D.; Sinclair, R.; King, L. A.; Jaramillo, T. F., Characterization of a Dynamic Y2Ir2O7 Catalyst during the Oxygen Evolution Reaction in Acid. *J. Phys. Chem. C* **2022,** *126*, 1751-1760.

(49) Luke, S.; Chatti, M.; Yadav, A.; Kerr, B. V.; Kangsabanik, J.; Williams, T.; Cherepanov, P. V.; Johannessen, B.; Tanksale, A.; MacFarlane, D. R.; Hocking, R. K.; Alam, A.; Yella, A.; Simonov, A. N., Mixed metal–antimony oxide nanocomposites: low pH water oxidation electrocatalysts with outstanding durability at ambient and elevated temperatures. *J. Mater. Chem. A* **2021,** *9*, 27468-27484.

(50) Wen, Y.; Chen, P.; Wang, L.; Li, S.; Wang, Z.; Abed, J.; Mao, X.; Min, Y.; Dinh, C. T.; Luna, P. D.; Huang, R.; Zhang, L.; Wang, L.; Wang, L.; Nielsen, R. J.; Li, H.; Zhuang, T.; Ke, C.; Voznyy, O.; Hu, Y.; Li, Y.; Goddard Iii, W. A.; Zhang, B.; Peng, H.; Sargent, E. H., Stabilizing Highly Active Ru Sites by Suppressing Lattice Oxygen Participation in Acidic Water Oxidation. *J. Am. Chem. Soc.* **2021,** *143*, 6482-6490.

(51) Simondson, D.; Chatti, M.; Gardiner, J. L.; Kerr, B. V.; Hoogeveen, D. A.; Cherepanov, P. V.; Kuschnerus, I. C.; Nguyen, T. D.; Johannessen, B.; Chang, S. L. Y.; MacFarlane, D. R.; Hocking, R. K.; Simonov, A. N., Mixed Silver–Bismuth Oxides: A Robust Oxygen Evolution Catalyst Operating at Low pH and Elevated Temperatures. *ACS Catal.* **2022,** *12*, 12912-12926.

(52) Wagman, D. D., *Technical Note 270, Washington, National Bureau of Standards*. 1968-1971.

(53) Frydendal, R.; Paoli, E. A.; Chorkendorff, I.; Rossmeisl, J.; Stephens, I. E. L., Toward an Active and Stable Catalyst for Oxygen Evolution in Acidic Media: Ti-Stabilized MnO2. *Adv. Energy Mater.* **2015,** *5*, 1500991-1500999.

(54) Zhou, L.; Shinde, A.; Montoya, J. H.; Singh, A.; Gul, S.; Yano, J.; Ye, Y.; Crumlin, E. J.; Richter, M. H.; Cooper, J. K.; Stein, H. S.; Haber, J. A.; Persson, K. A.; Gregoire, J. M., Rutile Alloys in the Mn–Sb–O System Stabilize Mn3+ To Enable Oxygen Evolution in Strong Acid. *ACS Catal.* **2018,** *8*, 10938-10948.

(55) Moreno-Hernandez, I. A.; MacFarland, C. A.; Read, C. G.; Papadantonakis, K. M.; Brunschwig, B. S.; Lewis, N. S., Crystalline nickel manganese antimonate as a stable water-oxidation catalyst in aqueous 1.0 M H2SO4. *Energy Environ. Sci.* **2017,** *10*, 2103-2108.

(56) Li, N.; Keane, T. P.; Veroneau, S. S.; Hadt, R. G.; Hayes, D.; Chen, L. X.; Nocera, D. G., Template-stabilized oxidic nickel oxygen evolution catalysts. *Proc. Natl. Acad. Sci.* **2020,** *117*, 16187-16192.

(57) Chong, L.; Gao, G.; Wen, J.; Li, H.; Xu, H.; Green, Z.; Sugar, J. D.; Kropf, A. J.; Xu, W.; Lin, X.-M.; Xu, H.; Wang, L.-W.; Liu, D.-J., La- and Mn-doped cobalt spinel oxygen evolution catalyst for proton exchange membrane electrolysis. *Science* **2023,** *380*, 609-616.

(58) Mondschein, J. S.; Callejas, J. F.; Read, C. G.; Chen, J. Y. C.; Holder, C. F.; Badding, C. K.; Schaak, R. E., Crystalline Cobalt Oxide Films for Sustained Electrocatalytic Oxygen Evolution under Strongly Acidic Conditions. *Chem. Mater.* **2017,** *29*, 950-957.

(59) Yu, J.; Garcés-Pineda, F. A.; González-Cobos, J.; Peña-Díaz, M.; Rogero, C.; Giménez, S.; Spadaro, M. C.; Arbiol, J.; Barja, S.; Galán-Mascarós, J. R., Sustainable oxygen evolution electrocatalysis in aqueous 1 M H2SO4 with earth abundant nanostructured Co3O4. *Nat. Commun.* **2022,** *13*, 4341.

(60) Li, A.; Kong, S.; Guo, C.; Ooka, H.; Adachi, K.; Hashizume, D.; Jiang, Q.; Han, H.; Xiao, J.; Nakamura, R., Enhancing the stability of cobalt spinel oxide towards sustainable oxygen evolution in acid. *Nat. Catal.* **2022,** *5*, 109-118.

(61) Schäfer, H.; Küpper, K.; Müller-Buschbaum, K.; Daum, D.; Steinhart, M.; Wollschläger, J.; Krupp, U.; Schmidt, M.; Han, W.; Stangl, J., Electro-oxidation of a cobalt based steel in LiOH: a non-noble metal based electro-catalyst suitable for durable water-splitting in an acidic milieu. *Nanoscale* **2017,** *9*, 17829-17838.

(62) Wang, N.; Ou, P.; Miao, R. K.; Chang, Y.; Wang, Z.; Hung, S.-F.; Abed, J.; Ozden, A.; Chen, H.-Y.; Wu, H.-L.; Huang, J. E.; Zhou, D.; Ni, W.; Fan, L.; Yan, Y.; Peng, T.; Sinton, D.; Liu, Y.; Liang, H.; Sargent, E. H., Doping Shortens the Metal/Metal Distance and Promotes OH Coverage in Non-Noble Acidic Oxygen Evolution Reaction Catalysts. *J. Am. Chem. Soc.* **2023,** *145*, 7829-7836.

(63) Shen, B.; He, Y.; He, Z.; Wang, Z.; Jiang, Y.; Gao, H., Porous Fe5Si3 intermetallic anode for the oxygen evolution reaction in acidic electrolytes. *J. Colloid Interf. Sci* **2022,** *605*, 637-647.

(64) Milosevic, M.; Böhm, T.; Körner, A.; Bierling, M.; Winkelmann, L.; Ehelebe, K.; Hutzler, A.; Suermann, M.; Thiele, S.; Cherevko, S., In Search of Lost Iridium: Quantification of Anode

Catalyst Layer Dissolution in Proton Exchange Membrane Water Electrolyzers. *ACS Energy Lett.* **2023**, 2682-2688.

(65) Cherevko, S.; Topalov, A. A.; Zeradjanin, A. R.; Keeley, G. P.; Mayrhofer, K. J. J., Temperature-Dependent Dissolution of Polycrystalline Platinum in Sulfuric Acid Electrolyte. *Electrocatalysis* **2014,** *5*, 235-240.

(66) Kasian, O.; Geiger, S.; Stock, P.; Polymeros, G.; Breitbach, B.; Savan, A.; Ludwig, A.; Cherevko, S.; Mayrhofer, K. J. J., On the Origin of the Improved Ruthenium Stability in RuO2–IrO2 Mixed Oxides. *J. Electrochem. Soc.* **2016,** *163*, F3099-F3104.

(67) Mom, R. V.; Falling, L. J.; Kasian, O.; Algara-Siller, G.; Teschner, D.; Crabtree, R. H.; Knop-Gericke, A.; Mayrhofer, K. J. J.; Velasco-Vélez, J.-J.; Jones, T. E., Operando Structure–Activity–Stability Relationship of Iridium Oxides during the Oxygen Evolution Reaction. *ACS Catal.* **2022,** *12*, 5174-5184.

(68) Mondschein, J. S.; Kumar, K.; Holder, C. F.; Seth, K.; Kim, H.; Schaak, R. E., Intermetallic Ni2Ta Electrocatalyst for the Oxygen Evolution Reaction in Highly Acidic Electrolytes. *Inorg. Chem.* **2018,** *57*, 6010-6015.

(69) Kwong, W. L.; Lee, C. C.; Shchukarev, A.; Björn, E.; Messinger, J., High-performance iron (III) oxide electrocatalyst for water oxidation in strongly acidic media. *J. Catal.* **2018,** *365*, 29-35.

(70) Etzi Coller Pascuzzi, M.; van Velzen, M.; Hofmann, J. P.; Hensen, E. J. M., On the Stability of Co3O4 Oxygen Evolution Electrocatalysts in Acid. *ChemCatChem* **2021,** *13*, 459-467.

(71) Geiger, S.; Kasian, O.; Shrestha, B. R.; Mingers, A. M.; Mayrhofer, K. J. J.; Cherevko, S., Activity and Stability of Electrochemically and Thermally Treated Iridium for the Oxygen Evolution Reaction. *J. Electrochem. Soc.* **2016,** *163*, F3132-F3138.

(72) Ledendecker, M.; Geiger, S.; Hengge, K.; Lim, J.; Cherevko, S.; Mingers, A. M.; Göhl, D.; Fortunato, G. V.; Jalalpoor, D.; Schüth, F.; Scheu, C.; Mayrhofer, K. J. J., Towards maximized utilization of iridium for the acidic oxygen evolution reaction. *Nano Research* **2019,** *12*, 2275-2280.

(73) Chang, S. H.; Danilovic, N.; Chang, K.-C.; Subbaraman, R.; Paulikas, A. P.; Fong, D. D.; Highland, M. J.; Baldo, P. M.; Stamenkovic, V. R.; Freeland, J. W.; Eastman, J. A.; Markovic, N. M., Functional links between stability and reactivity of strontium ruthenate single crystals during oxygen evolution. *Nat. Commun.* **2014,** *5*, 4191.

(74) Haraldsted, J.-P. B.; Révay, Z.; Frydendal, R.; Verdaguer-Casadevall, A.; Rossmeisl, J.; Kibsgaard, J.; Chorkendorff, I., Trace anodic migration of iridium and titanium ions and subsequent cathodic selectivity degradation in acid electrolysis systems. *Materials Today Energy* **2019,** *14*, 100352.

(75) Qiucheng Xu, S. G., Asger Moss, Marta Mirolo, Ib Chorkendorff, Jakub Drnec, Brian Seger, Identifying and alleviating the durability challenges in membrane-electrode-assembly devices for high-rate CO electrolysis. *PREPRINT (Version 1) available at Research Square [https://doi.org/10.21203/rs.3.rs-2491212/v1]* **2023**.

SYNOPSIS (Word Style "SN_Synopsis_TOC").